31st Annual International Conference of the IEEE EMBS
Minneapolis, Minnesota, USA, September 2-6, 2009

Three-dimensional High-resolution Optical Coherence Tomography (OCT) Imaging of Human Kidney

Qian Li[1], Maristela Onozato[2], Peter M. Andrews[2], Andrew Paek[1], Anik Duttaroy[1], Bobak Shirmahamoodi[1], James Jiang[3], Alex Cable[3], Yu Chen[1]
[1]Fischell Department of Bioengineering, University of Maryland, College Park, MD 20742
[2]Georgetown University School of Medicine, Washington, DC 20007
[3]Thorlabs Inc., Newton, NJ 07860

Abstract—**Optical coherence tomography (OCT) is a rapidly emerging imaging modality that can non-invasively provide cross-sectional, high-resolution images of tissue morphology *in situ* and in real-time. Previous studies have demonstrated that OCT is capable of accurately visualizing the pathological changes in the living kidney *in vivo* using the Munich–Wistar rat model. In this work, we establish, for the first time, the capability of OCT to image the intact human kidney *ex vivo*. Characteristic kidney anatomic structures including the blood vessels, uriniferous tubules, glomeruli, and kidney capsules can be readily discerned. The diameter and volume parameters of these structures can also be automatically quantified. These two parameters may be critical in clinical applications such as the assessment of the donor kidney's viability prior to transplantation, or image the kidney responses to ischemic insult.**

I. Introduction

Optical coherence tomography (OCT) is a high-resolution, cross-sectional, three-dimensional imaging modality that measures the echo delay of light to generate images [1]. Although the light scattering properties of biological tissue typically limit light penetration to less than 2 mm, this imaging depth has proven sufficient to provide valuable information about tissue pathology in a number of biomedical fields including ophthalmology [2], cardiology [3], and gastroenterology [4], [5]. OCT can be interfaced with various imaging devices such as catheters, endoscopes, laparoscopes, and needles, with typical image resolutions of 1-15 μm [6]. Therefore, OCT will be a promising imaging modality to assess tissue pathologies *in situ* and in real time.

One potential but under-explored OCT application is to evaluate the viability of donor kidneys [7]. The kidney is one of the most important organs in the human body. Blood vessels, uriniferous tubules, and glomeruli perform basic functions in the kidney. For example, glomeruli, which are cluster of tiny blood vessels (capillaries) filters and allows water and soluble wastes to pass through. Previous study indicated that proximal tubular structure and post-transplant viability are closely correlated [8]. In recent studies, living rat kidneys were observed *in vivo* before, during, and after an ischemic insult [9]. OCT imaging enabled visualization of the morphology of blood vessels, uriniferous tubules, and glomeruli. Three-dimensional measurement provided quantitative evaluations of the volume changes in tubular lumens in response to renal ischemia. OCT represents an exciting new approach to visualize, in real-time, the pathological changes in the living kidney in a minimally-invasive fashion.

The purpose of this study is to investigate the ability of OCT to image human kidney morphology, which is an important step before translating this promising technology to clinical applications. Past studies, such as the above mentioned, have been successfully performed in animal models. Although these foregoing studies demonstrated the ability of OCT to image rat kidney pathology *in situ*, if OCT is to be used for the assessment of the donor kidney prior to its transplantation, its applicability to image the human kidney in real-time, such as imaging resolution, penetration depth, and the capability to reveal human kidney microanatomy, must be evaluated.

II. Materials and Methods

A. Human Kidney and Histology

This study protocol has been approved by the Institutional Review Boards (IRB) at both the University of Maryland and Georgetown University. Four donor kidneys were obtained through the Washington Regional Transplant Consortium (WRTC). Upon arrival, the kidneys were fixed by vascular perfusion with 10% neutral formalin (through the renal artery) to preserve their renal morphology. After the OCT image acquisition, the location and direction of each scanned section were marked with ink, for subsequent standard histology processing. A serial of 4 μm thick sections were cut, stained with hematoxylin-eosin (H&E), and photographed with a Nikon Eclipse 80i (Nikon, Melville, NY) attached to a digital camera Nikon DS-Fi1 (Nikon). The micrographs were obtained for comparison with OCT images.

B. Optical Coherence Tomography Imaging

A high-speed high-resolution OCT system (Thorlabs Inc., NJ, USA) using swept source/Fourier domain detection that enables three-dimensional (3D) OCT imaging *in situ* was used in this study. The light source was a wavelength-swept laser light source generating a 100 nm full width at half maximum (FWHM) bandwidth at approximately 1300 nm, yielding approximately 10 μm axial image resolution in the tissue. The laser operated at a swept rate of 16 kHz with an average output power of 12 mW. The imaging was performed using an OCT microscope setup with a frame rate of 30 frames per second.

Fig. 1 shows the overall schematic of the OCT system used in this experiment. The inset in the lower left corner of Fig. 1 shows the photo of the imaging instrument used in the experiment.

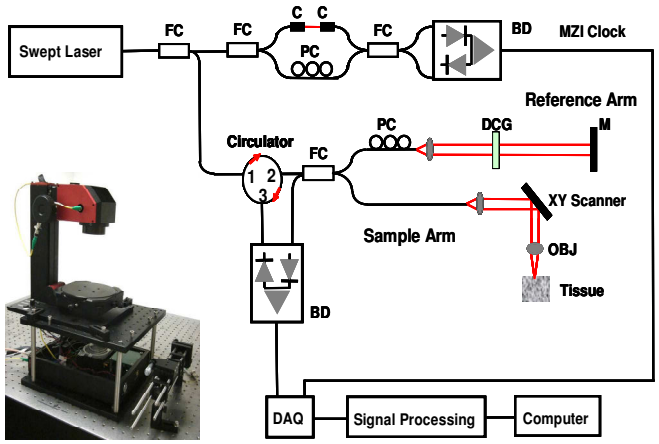

Fig. 1. FC: fiber coupler, PC: polarization controller, C: collimator, MZI: Mach-Zehnder interferometer (frequency clocks), M: mirror, BD: balanced detector, DAQ: data acquisition board, DCG: dispersion compensating glasses, OBJ: objective.

C. OCT Image Processing and Analysis

3D OCT images of the kidney measuring 2.5 mm by 2.5 mm by 2.5 mm (with 512 x 512 x 512 pixels) were obtained from various locations on the human kidneys within minutes, in a non-contact manner. To quantitatively evaluate the OCT images and obtain diagnostic information, image processing was performed on the individual cross-sectional (XZ plane) OCT images. Fig. 2 displays a flow chart of the imaging processing algorithm.

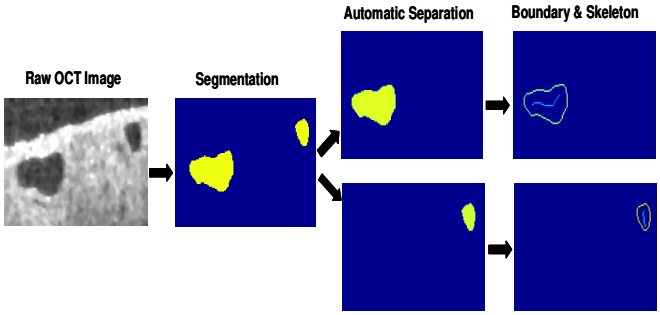

Fig. 2. General flow chart of the automatic image processing algorithm, which includes four major steps: 1) image segmentation from the raw OCT image; 2) automatic region separation and selection; 3) finding the boundary and skeleton for each isolated regions to calculate the mean tubular diameter, and 4) sum all segmented regions to estimate the tubular volume. Computer estimated results have been validated with manual measurements.

The image processing included four major steps. First, the raw OCT image data were obtained. Then the structures in the OCT image (such as uriniferous tubules and vessels) were segmented from the kidney parenchyma based on their different backscattering intensities. Next, an intelligent image processing algorithm was used to automatically separate all the isolated sections (i.e. uriniferous tubules) from the segmented images. The algorithm systematically filled the region up to the section boundary and labeled each region with a unique index. This algorithm also allowed different regions to be individually selected and analyzed. The boundary and skeleton were subsequently generated for each isolated section. Finally, the sizes of those isolated sections were calculated based on averaging the shortest distances among the boundaries and skeletons. It was therefore possible to obtain all the individual segmented images as well as their dimensional information.

III. Results

Raw OCT image data were collected by the experiment instrumentation setup, and then visualized in real time. Images along the three orthogonal image-planes (XY, YZ, XZ) in the Euclidean space were displayed sequentially. Moreover, the rendering of the images provided a 3D volumetric view. The computed microstructure sizes were then added to the reconstructed images, revealing quantitative information of the kidney microanatomy.

The interested kidney microstructures including the uriniferous tubules, blood vessels, and glomeruli were identified based on their distinct morphologies. Comparisons between the OCT image and corresponding histological micrograph indicated a close match for regions of interests (ROI). In addition, the resolution of OCT images is proven to be comparable to that of conventional histopathology. Fig. 3a shows a representative cross-sectional OCT image of the human kidney, and Fig. 3b is the corresponding histopathology. It is clearly observed that OCT can penetrate through the kidney capsule (C) with a penetration depth of more than 0.8 mm. The kidney microanatomy including uriniferous tubules (T) and glomeruli (G) were also readily distinguished.

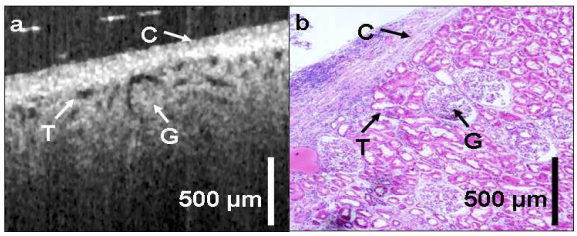

Fig. 3. (a) Cross-sectional OCT image of the human kidney. Uriniferous tubules (T), glomeruli (G) and the kidney capsule (C) are distinguishable. (b) Conventional histology of the associated area in the human kidney.

Fig. 4A is the three-dimensional view of the human kidney, as generated from the individual cross-sectional images. Fig. 4B, C, D show the representative images along the three orthogonal planes (XY, YZ, XZ), respectively. Detailed kidney vascular networks can be visualized in all the image planes.

For those regions without any microstructure, the light intensity decreases exponentially over the depth due to the light scattering effects. However, microstructures such as uriniferous tubules or blood vessels alter this exponentially change and reduce the light intensity to lower intensity levels, due to minimal light backscattering within these structures. After the light passes through these structures, the light continues decreasing exponentially again. This phenomenon results in relatively higher light intensity below some of the microstructures (Fig. 4C and D).

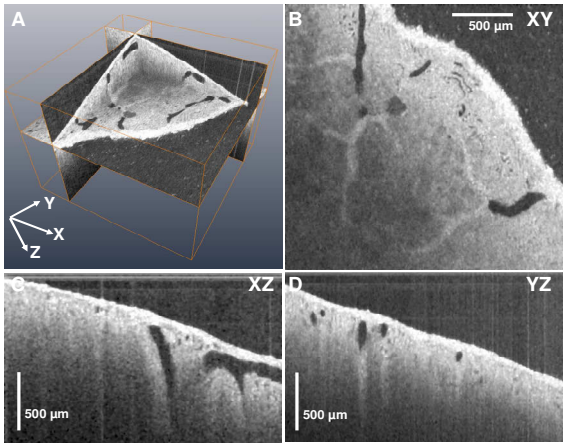

Fig. 4. (A) 3D cut-through view of the human kidney. The blood vessels as well as kidney parenchyma are visualized. (B) An OCT image slice-view in the XY plane. (C) An OCT image slice-view in the XZ plane. (D) An OCT image slice-view in the YZ plane.

The OCT image data set was further segmented and analyzed to quantify the luminal diameter of the blood vessels. Fig. 5A shows the 3D reconstruction images of the ROI with continuous blood vessels after intensity segmentation. The morphological features of the blood vessels can be comprehensively examined. Fig. 5B shows the quantification of the representative blood vessels luminal diameters. The vessel size ranges from 20 µm to 170 µm, as displayed by the color scale in Fig. 5B.

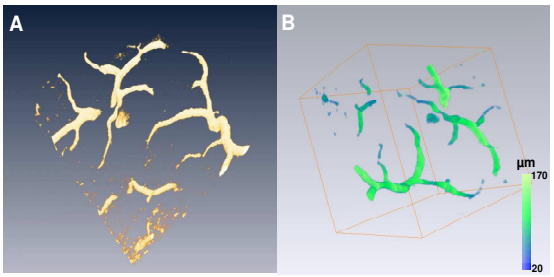

Fig. 5. (A) 3D vascular network segmented from OCT volumetric data. (B) 3D vascular network image reconstruction color-coded with dimension information.

From the segmented images, individual vessels can be isolated automatically by the image processing algorithms, and their diameters can be quantified. It is also possible to estimate the total blood vessel luminal volume from the segmented images. These two parameters (diameter and luminal volume) may be related to the physiological function of human kidney and could serve as the indicative parameters for assessment of transplant kidney viability. Future work will involve the quantification of those two parameters for different human kidneys, and compare them with the histopathology for diagnostic calibration.

IV. Discussion and Conclusion

We have demonstrated the capability of OCT imaging of human kidney microanatomy. The ability of OCT to provide 3D, high resolution imaging illustrates the potential of using OCT to image the donor kidney structures and to evaluate the organ viability, or image the responses to acute kidney injury.

Acknowledgement

This work is supported in part by the Nano-Biotechnology Award of the State of Maryland, the Minta Martin Foundation, the General Research Board (GRB) Award of the University of Maryland, UMB-UMCP Seed Grant Program, and the Prevent Cancer Foundation.

References

[1] D. Huang, E. A. Swanson, C. P. Lin, J. S. Schuman, W. G. Stinson, W. Chang, M. R. Hee, T. Flotte, K. Gregory, C. A. Puliafito, and J. G. Fujimoto, "Optical coherence tomography," Science, **254,** 1178-1181 (1991).

[2] J. S. Schuman, C. A. Puliafito, and J. G. Fujimoto, *Optical coherence tomography of ocular diseases (2nd Edition)*. 2004, Thorofare, NJ: Slack Inc.

[3] I. K. Jang, B. Bouma, B. MacNeill, M. Takano, M. Shishkov, N. Iftima, and G. J. Tearney, "In-vivo coronary plaque characteristics in patients with various clinical presentations using Optical Coherence Tomography," Circulation, **108,** 373-373 (2003).

[4] Y. Chen, A. D. Aguirre, P. L. Hsiung, S. Desai, P. R. Herz, M. Pedrosa, Q. Huang, M. Figueiredo, S. W. Huang, A. Koski, J. M. Schmitt, J. G. Fujimoto, and H. Mashimo, "Ultrahigh resolution optical coherence tomography of Barrett's esophagus: preliminary descriptive clinical study correlating images with histology," Endoscopy, **39,** 599-605 (2007).

[5] J. A. Evans, J. M. Poneros, B. E. Bouma, J. Bressner, E. F. Halpern, M. Shishkov, G. Y. Lauwers, M. Mino-Kenudson, N. S. Nishioka, and G. J. Tearney, "Optical coherence tomography to identify intramucosal carcinoma and high-grade dysplasia in Barrett's esophagus," Clinical Gastroenterology and Hepatology, **4,** 38-43 (2006).

[6] J. G. Fujimoto, "Optical coherence tomography for ultrahigh resolution in vivo imaging," Nature Biotechnology, **21,** 1361-1367 (2003).

[7] Y. Chen, P. M. Andrews, A. D. Aguirre, J. M. Schmitt, and J. G. Fujimoto, "High-resolution three-dimensional optical coherence tomography imaging of kidney microanatomy ex vivo," Journal of biomedical optics, **12,** 034008 (2007).

[8] P. M. Andrews, B. S. Khirabadi, and B. C. Bengs, "Using tandem scanning confocal microscopy to predict the status of donor kidneys," Nephron, **91,** 148-55 (2002).

[9] P. M. Andrews, Y. Chen, M. L. Onozato, S. W. Huang, D. C. Adler, R. A. Huber, J. Jiang, S. E. Barry, A. E. Cable, and J. G. Fujimoto, "High-resolution optical coherence tomography imaging of the living kidney," Laboratory investigation; a journal of technical methods and pathology, **88,** 441-9 (2008).